Organic & Biomolecular Chemistry

Cite this: *Org. Biomol. Chem.*, 2012, **10**, 2035

www.rsc.org/obc

PAPER

Synthesis and photooxidation of oligodeoxynucleotides containing 5-dimethylaminocytosine as an efficient hole-trapping site in the positive-charge transfer through DNA duplexes†

Hisatsugu Yamada,*[a] Masayuki Kurata,[b] Kazuhito Tanabe,[b] Takeo Ito[b] and Sei-ichi Nishimoto*[b]

Received 27th September 2011, Accepted 12th December 2011
DOI: 10.1039/c2ob06642d

We have designed and synthesized DNA duplexes containing 5-dimethylaminocytosine (^{DMA}C) to investigate the effects of C(5)-substituted cytosine bases on the transfer and trapping of positive charge (holes) in DNA duplexes. Fluorescence quenching experiments revealed that a ^{DMA}C base is more readily one-electron oxidized into a radical cation intermediate as compared with other natural nucleobases. Upon photoirradiation of the duplexes containing ^{DMA}C, the photosensitizer-injected hole migrated through the DNA bases and was trapped efficiently at the ^{DMA}C sites, where an enhanced oxidative strand cleavage occurred by hot piperidine treatment. The ^{DMA}C radical cation formed by hole transfer may undergo specific hydration and subsequent addition of molecular oxygen, thereby leading to its decomposition followed by a predominant strand cleavage at the ^{DMA}C site. This remarkable property suggests that the modified cytosine ^{DMA}C can function as an efficient hole-trapping site in the positive-charge transfer in DNA duplexes.

Introduction

Photosensitized oxidation of DNA has been studied extensively in relation to the positive-charge (hole) transfer through DNA.[1–3] In general, photosensitized one-electron oxidation of DNA can form a primary base radical cation, the positive charge of which migrates through the π-stack of DNA base pairs to produce oxidative cleavage of a DNA strand at specific base with the lowest oxidation potential such as consecutive guanine (G) sites.[3] It has been demonstrated that a hole generated in DNA can migrate over a 20–30 nm range under certain conditions.[1,4] Hole transfer through DNA has attracted particular interest in view of potential application of its properties to gene analysis of mutation and molecular wires in nanoscale electronic devices.[5,6]

A wide variety of modified nucleobases have been developed for investigating and promoting the hole transfer reaction in DNA duplexes.[7–15] Recent studies on hole transfer in photosensitizer-tethered DNA duplexes showed that introduction of modified purine bases into DNA can dramatically promote the photosensitizer injected hole transfer efficiency.[7,8] These strategies provide useful information for better mechanistic understanding as well as the application of hole-transfer to DNA-based nanomaterials. On the other hand, modified purine bases such as 7-deazaguanine,[9] 8-methoxyguanine,[10] and 2-amino-7-deazaadenine[11] can thermally trap the hole that was injected and migrated through the DNA duplex. These modified nucleobases have also been used as effective tools for investigating long-range hole transfer through DNA duplexes. Other examples are *N*-cyclopropyl-modified purine bases that kinetically trap the hole migrating along the DNA duplex.[12,13] In contrast to various types of modified purine bases reported so far, there have been limited examples of chemically modified pyrimidine bases possessing a hole trapping ability, *e.g.*, *N*(4)-cyclopropyl-modified cytosine that kinetically traps holes migrating along the DNA duplex[14] and trimethoxyphenyl-substituted uracil that thermally traps holes induced by ionizing radiation.[15] In this context, development of an efficient hole-trapping pyrimidine base is an intriguing area of research for further understanding of the mechanism by which hole migrates through a duplex of DNA containing diverse sequences.

In this study, we have developed DNA duplexes containing 5-dimethylaminocytosine (^{DMA}C) as a novel electron-donating nucleobase and characterized the hole-transfer reactions in DNA possessing modified base sites of ^{DMA}C. Fluorescence quenching experiments suggested that incorporation of the dimethylamino group into the C(5) position of cytosine significantly decreases

[a]*Advanced Biomedical Engineering Research Unit, Kyoto University, Katsura, Nishikyo-ku, Kyoto 615-8510, Japan. E-mail: yamada.hisatsugu.3r@kyoto-u.ac.jp; Fax: +81-75-383-2805; Tel: +81-75-383-7554*
[b]*Department of Energy and Hydrocarbon Chemistry, Graduate School of Engineering, Kyoto University, Katsura, Kyoto 615-8510, Japan. E-mail: nishimot@scl.kyoto-u.ac.jp; Fax: +81-75-383-2501; Tel: +81-75-383-2500*

†Electronic supplementary information (ESI) available: synthesis, Stern–Volmer plots of fluorescence quenching, PAGE analysis, and ESI-TOF mass analysis. See DOI: 10.1039/c2ob06642d

the oxidation potential of ^{DMA}C because of a strong electron-donating effect of a dimethylamino group. Gel electrophoresis analysis revealed that a photoinjected hole migrates through the DNA bases to be trapped efficiently at the ^{DMA}C site, where enhanced oxidative strand cleavage was induced. Thus, ^{DMA}C can function as an effective hole-trapping site, thereby probing the hole transfer reaction in DNA.

Results and discussion

Electron transfer oxidation property of ^{DMA}C

We evaluated the one-electron oxidation property of ^{DMA}C using a Stern–Volmer analysis of the fluorescence quenching by monomeric ^{DMA}C (5-dimethylamino-2′-deoxycytidine, $d^{DMA}C$), which was prepared from 5-bromo-2′-deoxycytidine with dimethylamine (see ESI†). 9,10-Dicyanoanthracene (DCA) was employed as a photooxidizing fluorophore for this analysis. It has sufficient reduction potential (1.95 V *versus* NHE in the singlet excited state) to oxidize all of the naturally occurring nucleobases.[16a] Similar analysis has been widely used for investigation of the one-electron oxidation process of DNA bases.[16]

Upon electronic excitation of DCA at 390 nm in deoxygenated buffer solution, the intensity of the fluorescence emission decreased with increasing concentrations of $d^{DMA}C$. The fluorescence quenching rate constant (k_q) of the singlet excited state, ^{1}DCA*, was determined by the Stern–Volmer plots of the fluorescence spectral data (see Fig. S1†) in conjunction with the fluorescence lifetime of ^{1}DCA*.[17] As summarized in Table 1, $d^{DMA}C$ showed the highest k_q value for the fluorescence quenching of ^{1}DCA* ($k_q = 6.5 \times 10^9$ M^{-1} s^{-1}) among the 2′-deoxyribonucleosides evaluated: the k_q values of 2′-deoxycytidine (dC), thymidine (dT), 2′-deoxyadenosine (dA), and 2′-deoxyguanosine (dG) were 2.9, 3.2, 4.6, and 5.6×10^9 M^{-1} s^{-1}, respectively. These results strongly suggest that ^{DMA}C is more readily one-electron oxidized into a radical cation intermediate than any other natural nucleobases. Therefore, ^{DMA}C can function as an electron-donating site, where a hole (radical cation) migrating through DNA is localized.

Table 1 Fluorescence quenching rate constants (k_q) of DCA with 2′-deoxyribonucleosides[a]

2′-Deoxyribonucleosides	k_q ($\times 10^9$ $M^{-1}s^{-1}$)[b]
$d^{DMA}C$	6.5
dG	5.6
dA	4.6
dT	3.2
dC	2.9

[a] The excitation wavelength for DCA (25 μM) was 390 nm. Relative intensity of the emission band at 487 nm was measured in the presence of 25 μM DCA, in deoxygenated solution of 20 mM phosphate buffer (pH 7.0). [b] The dynamic quenching rate constant k_q was determined by the Stern–Volmer equation: $I_0/I = 1 + k_q\tau_0$[2′-deoxyribonucleoside], where I_0/I is the ratio of the emission intensities in the absence and presence of 2′-deoxyribonucleoside and τ_0 is the lifetime of the singlet excited state of DCA (15.1 ns)[17] in the absence of quencher.

Synthesis and thermal stability of ^{DMA}C-containing ODNs duplex

Scheme 1 shows the synthesis of oligodeoxynucleotides (ODNs) containing ^{DMA}C. 5-Bromo-2′-deoxyuridine protected by a 4,4′-dimethoxytrityl group (**1**) was converted to **2** by treatment with 50% dimethylamine. The 3′-hydroxyl group of **2** was then protected to afford 5-dimethylamino-2′-deoxyuridine derivative (**3**). The 4-oxo group of the resulting **3** was transformed to an amino group to give the ^{DMA}C derivative (**4**) in two steps. *N*-Acetyl-protected ^{DMA}C (**6**) was prepared from **4** by standard acetyl protection of the exocyclic amine and subsequent desilylation of the hydroxy group, then converted into ^{DMA}C phosphoramidite derivative (**7**) which was incorporated into DNA using a DNA synthesizer and conventional phosphoramidite chemistry. Our choice of the photosensitizer was 9,10-anthraquinone (AQ), which is well known to induce hole injection to the adjacent DNA bases and thereafter positive-charge transfer through the DNA duplex.[18] ODNs with AQ sensitizer were similarly prepared from a prescribed phosphoramidite derivative as in previously reported methods.[18b] The ODNs used in this study are summarized in Fig. 1a.

The thermal stability of ^{DMA}C-containing duplexes was evaluated by monitoring the melting temperatures (T_m) in 10 mM sodium cacodylate buffer (pH 7.0) containing 100 mM NaCl (Fig. 1b). Introduction of the AQ moiety slightly enhanced the thermal stability of the duplex because of the π-stacking effect between the hydrophobic planar ring of AQ and the flanking bases. The T_m of the AQ-ODN1(G)/ODN1(^{DMA}C) duplex (T_m = 57.0 °C) was only slightly different from that of a reference duplex AQ-ODN1(G)/ODN1(C) (T_m = 56.9 °C). The circular dichroism (CD) spectra for each duplex showed a positive peak at 274 nm and a negative peak at 249 nm (Fig. 1c), indicating that the global structure of the AQ-ODN1(G)/ODN1(^{DMA}C) duplex was retained as a characteristic B-form. These results suggest that the dimethylamino group of ^{DMA}C oriented toward the major groove does not significantly perturb the duplex structure.

Hole trapping at ^{DMA}C in the positive-charge transfer through DNA duplex

We also investigated the hole-transfer and hole-trapping properties of AQ-tethered DNA duplexes possessing a ^{DMA}C base in the middle spot of the sequence. Hole injection into the duplex was induced upon photoexcitation of AQ at the 5′-end of the duplex. The duplex consisting of AQ-ODN1(G) with ^{32}P-labeled ODN1(^{DMA}C) in sodium cacodylate buffer solution (pH = 7.0) was photoirradiated (365 nm) at 20 °C. The photoirradiated samples were treated with hot piperidine and subjected to polyacrylamide gel electrophoresis (PAGE). The results are shown in Fig. 2a and 2b.

A predominant strand cleavage at the ^{DMA}C site was observed in the ODN1(^{DMA}C)/AQ-ODN1(G) duplex, whereas relatively weak strand cleavage occurred at the 5′-G_{14} site of a G-doublet, which is well known as an efficient hole-trapping site[3] (Fig. 2a, lanes 2–4). The cleavage yields at the ^{DMA}C site and G_{14} site were 21% and 10%, respectively, after 20-min photoirradiation (Fig. 2b). No strand cleavage band was observed at the ^{DMA}C

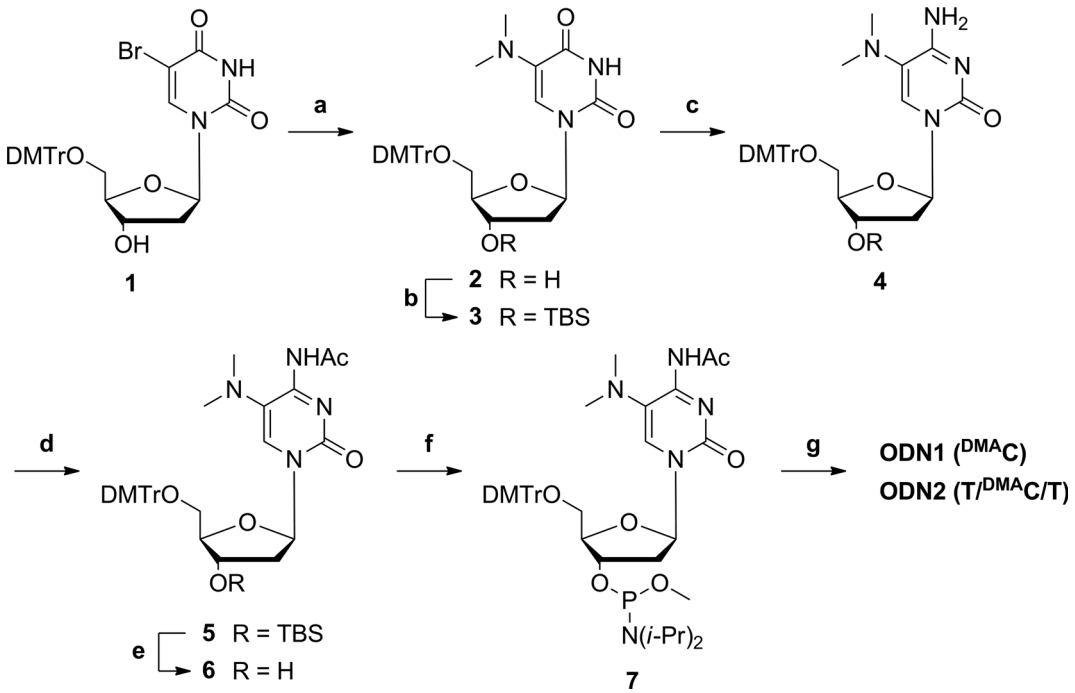

Scheme 1 Reagents and conditions: a) 50% aqueous dimethylamine, 60 °C, 60 h, 52%; b) *tert*-butyldimethylsilylchloride, imidazole, DMF, r.t., 6 h, 93%; c) 2,4,6-triisopropylbenzenesulfonyl chloride, DMAP, Et_3N, CH_3CN, r.t., 16 h, and then 28% aqueous NH_3, 0 °C to r.t., 3 h, 57%; d) acetic anhydride, DMAP, pyridine, r.t., 12 h, 92%; e) TBAF, THF, r.t., 1 h, 80%; f) *N*,*N*-diisopropylmethylphosphonamidic chloride, DIPEA, CH_3CN, r.t., 4 h, quant. g) automated DNA synthesis.

site in a control duplex without an AQ (Fig. 2a, lanes 6–9), indicating that strand cleavage at the ^{DMA}C due to possible direct photolysis is negligible under the present conditions.[19] In the absence of piperidine treatment after photoirradiation, the strand cleavage was significantly suppressed (Fig. 2a, lane 5). These results clearly indicate that a given DNA base radical cation (hole) induced by the excited AQ migrates through the DNA duplex to be trapped efficiently at the ^{DMA}C base rather than the 5′-G site of a G-doublet. Similarly, separate experiments using the ODN2($X_1/X_2/X_3$)/AQ-ODN2($Y_1/Y_2/Y_3$) duplexes showed that the cleavage efficiency of the ^{DMA}C sites in ODN2(T/^{DMA}C/T)/AQ-ODN2(A/G/A) were significantly higher than that of the corresponding 5′-G site in ODN2(T/G/G)/AQ-ODN2(C/C/A) (see Fig. S2†) and that of the middle of the G triplet in ODN2(G/G/G)/AQ-ODN2(C/C/C) (see Fig. S3†) arranged at the same distance from AQ.

It has been suggested that the hole transfer through DNA involves a short-range charge-transfer process between G or A bases, which are known to have the highest HOMO (highest occupied molecular orbital) energy levels among the naturally occurring nucleobases.[1–3] In this context, competitive localization of the migrating hole at the complementary base is possibly involved in the hole trapping at ^{DMA}C. In addition, Kawai and co-workers have reported that the oxidation potential of G can be regulated by introducing a substituent to cytosine on the complementary strand.[20] In this view, we examined the effects of complementary bases on the strand cleavage efficiency at ^{DMA}C. Hypoxanthine (I), which has a higher oxidation potential (E_{ox} = 1.50 V *versus* NHE)[21] than that of G (E_{ox} = 1.29 V *versus* NHE),[22] was introduced into the complementary strand (AQ-ODN1(I)). The cleavage efficiency at ^{DMA}C was compared relative to the AQ-ODN1(G) duplex. As shown in Fig. 2c, cleavage efficiencies at ^{DMA}C sites in AQ-ODN1(I)/ODN1(^{DMA}C) were virtually identical to that in the AQ-ODN1(G)/ODN1(^{DMA}C), indicating that the oxidation potentials of complementary bases have little effect on the strand cleavage at ^{DMA}C. In light of the Stern–Volmer analysis data (Table 1), this suggests that a photoinjected and migrated hole may be localized at the ^{DMA}C site rather than its complementary base, which further supports the idea that ^{DMA}C can function as an efficient electron donor for hole transfer through DNA duplexes.

LC/ESI-TOF mass analysis in the one-electron photooxidation of d^{DMA}C to get a mechanistic insight into photooxidation and strand cleavage of ^{DMA}C

For a mechanistic understanding of the one-electron oxidation and piperidine-induced strand cleavage at ^{DMA}C, we carried out the LC/ESI-TOF mass analysis in the one-electron oxidation of d^{DMA}C induced by photoexcited riboflavin, which has been reported to predominantly sensitize a Type I photooxidation.[23] Aerobic solutions of d^{DMA}C (200 μM) and riboflavin (200 μM) in 2 mM sodium cacodylate buffer (pH 7.0) containing 10 mM NaCl were photoirradiated with 365 nm UV light, and the reaction was analyzed by LC/ESI–MS. The results are shown in Fig. 3. After 2 min irradiation, the HPLC profile exhibited two major peaks at 1.9 and 3.4 min along with the degradation of d^{DMA}C (Fig. 3a). Upon prolonged photoirradiation (*ca.* 10 min), d^{DMA}C was completely degraded, while the peak intensity at 3.4 min decreased with an increase in the peak at 1.9 min. The ESI–MS analyses of these characteristic LC peaks indicates

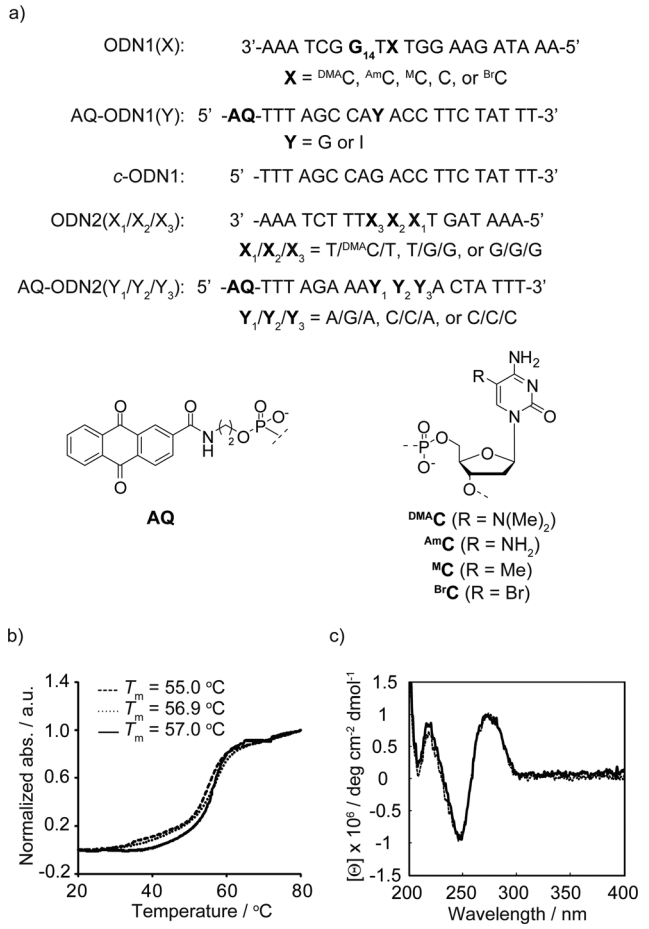

Fig. 1 (a) Sequences and structures of ODNs used in this study. ^{DMA}C, ^{Am}C, ^{M}C, ^{Br}C, and I denote 5-dimethylaminocytosine, 5-aminocytosine, 5-methylcytosine, 5-bromocytosine, and hypoxanthine, respectively. (b) Normalized UV melting curve of the duplexes (1 μM strand concentration) measured at 260 nm in 10 mM sodium cacodylate buffer (pH 7.0) containing 100 mM NaCl: AQ-ODN1(G)/ODN1(^{DMA}C) (solid line), AQ-ODN1(G)/ODN1(C) (dotted line), and *c*-ODN1/ODN1(^{DMA}C) (dashed line). (c) CD spectra (5 μM strand concentration) of AQ-ODN1(G)/ODN1(^{DMA}C) (solid line) and AQ-ODN1(G)/ODN1(C) (dashed line) observed at 25 °C in 10 mM sodium cacodylate buffer (pH 7.0) containing 100 mM NaCl.

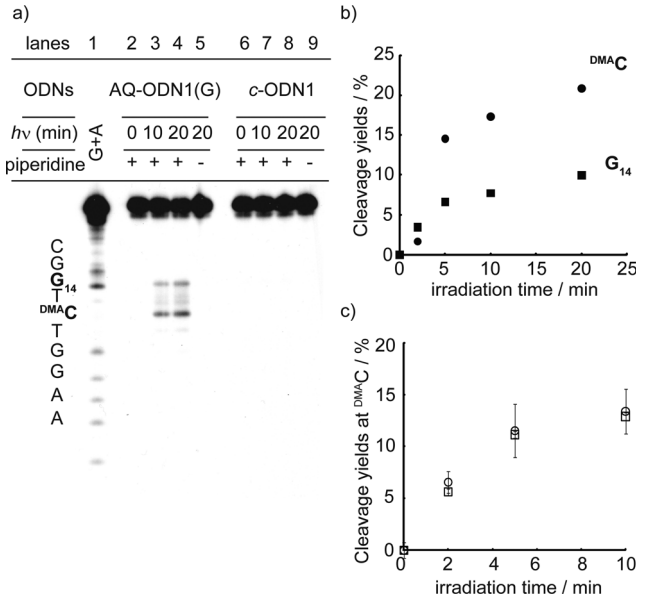

Fig. 2 (a) PAGE image of photoirradiated AQ-ODN1(G)/ODN1(^{DMA}C) (lanes 2–5) and *c*-ODN1/ODN1(^{DMA}C) (lanes 6–9). ODN duplexes in 10 mM sodium cacodylate buffer (pH 7.0) containing 100 mM NaCl were photoirradiated (365 nm, 0–20 min) at 20 °C, followed by piperidine treatment (90 °C, 20 min). The samples in lanes 5 and 9 were not treated with hot piperidine. G+A indicates Maxam–Gilbert sequencing lane (lane 1). (b) Strand cleavage yields at the ^{DMA}C site (closed circle) and the G_{14} site (closed square) in photoirradiated AQ-ODN1(G)/ODN1(^{DMA}C) estimated by densitometric analysis of the gel image. (c) Effects of the complementary base (Y = G or I in AQ-ODN1(Y)) on the strand cleavage yields of ^{DMA}C were determined by PAGE. AQ-ODN1(G)/ODN1(^{DMA}C) (open circle) and AQ-ODN1(I)/ODN1(^{DMA}C) (open square) were photoirradiated under conditions that otherwise were identical to those described above. Cleavage yields were calculated from the corresponding band intensities relative to the total intensity. Error bars represent the standard deviation of three independent measurements.

transient formation of unstable *N*-formylurea derivative (dNfu) (*m*/*z* 301.1172; calcd. for $[M - H]^-$ = 301.1148) (Fig. 3b, bottom) and its intramolecularly cyclized imidazolone derivative (dImz) (*m*/*z* 271.1223, 309.0989; calcd. for $[M - H]^-$ = 273.1199, $[M + Cl]^-$ = 309.0971) (Fig. 3b, top).[24,25]

Scheme 2 shows a plausible mechanism for one-electron oxidation and strand cleavage at ^{DMA}C. The primary step involves one-electron oxidation of ^{DMA}C into the corresponding radical cation ($^{DMA}C^{\cdot+}$) intermediate by way of AQ-injected hole transfer through DNA and subsequent hole trapping at the ^{DMA}C site. By reference to the proposed reaction mechanisms for one-electron oxidation of thymidine[26] and 2′-deoxycytidine,[27] the resulting $^{DMA}C^{\cdot+}$ may predominantly undergo specific hydration at C(6) to give a C(5)-yl radical intermediate, followed by addition of molecular oxygen at the C(5)-yl radical to afford C(5)-peroxyl radical intermediate that is converted to a C(5)-hydroperoxide.[28]

Cadet and co-workers have reported that 2′-deoxyribofuranosyl-5-hydroxy-5-methylhydantoin was formed from the hydrolytic decomposition of 6-hydroxy-5-hydroperoxy-5,6-dihydrothymidine (one of the oxidation products of dT) through the opening of the 1,6-pyrimidine ring.[26] In this light, the resulting C(5)-hydroperoxide intermediate of ^{DMA}C may undergo hydrolytic decomposition to give an imidazolone analogue (Imz), a related degradation product to 5-hydroxy-5-methylhydantoin, as in the case of dT photooxidation. Another pathway could also be considered: an *N*-formylurea analogue (Nfu) is likely to be generated by the dispropotionation of C(5)-peroxyl radical intermediate of ^{DMA}C.[29] The resulting Nfu may undergo hydrolysis of the formyl group and intramolecular cyclization to give an Imz analogue. However, the occurrence of the bi-molecular processes may be ruled out in the AQ-photosensitized oxidation of the ^{DMA}C site in the restricted structure of the DNA duplex.

An attempt was also made to investigate the photooxidation of the AQ-ODN1(G)/ODN1(^{DMA}C) duplex using ESI-TOF mass spectroscopy. The duplex (10 μM) in sodium cacodylate buffer solution (pH = 7.0) was photoirradiated (365 nm) at 20 °C for 20 min, and then subjected to ESI-TOF mass analysis. As shown in Fig. S4†, the mass spectral peak of *m*/*z* 1554.5 was observed,

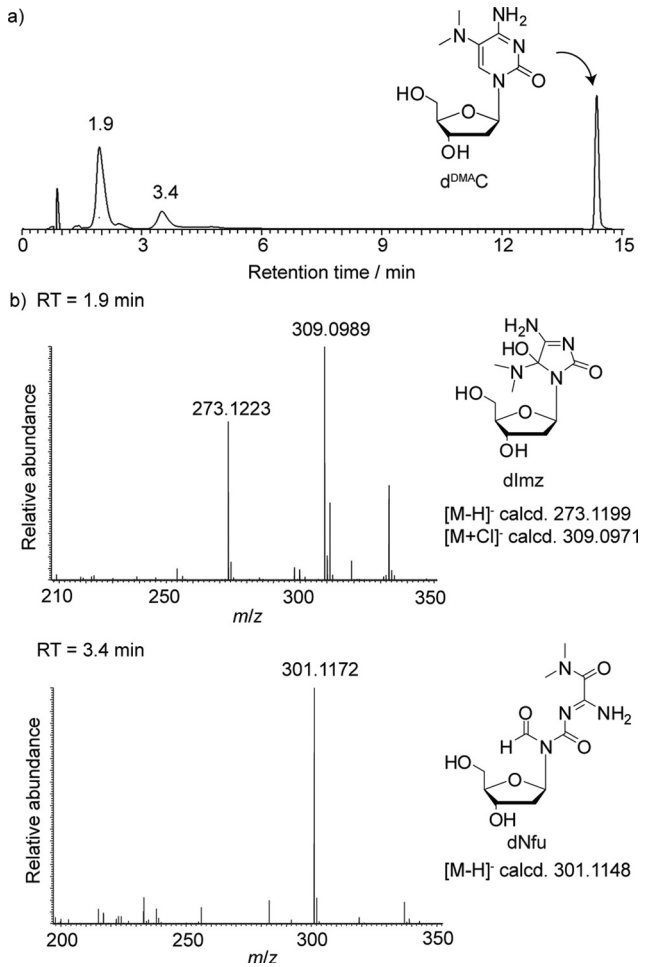

Fig. 3 LC/ESI–MS (negative mode) profiles of the photooxidation of $d^{DMA}C$ (200 μM) sensitized by riboflavin (200 μM) in 2 mM sodium cacodylate buffer (pH 7.0) containing 10 mM NaCl upon 365 nm photoirradiation at 0 °C. (a) Representative HPLC profiles of the reaction mixture after 2 min photoirradiation. The column eluents were monitored by UV absorbance at 260 nm. (b) LC/MS traces of the peaks at 1.9 min (top) and 3.4 min (bottom).

indicating the formation of oxidized ODN1(Imz) (calcd. for $[M - 4H]^{4-}$ = 1554.7). Irrespective of the reaction mechanisms, it is likely that a hole-trapped intermediate $^{DMA}C^{\cdot+}$ may be converted into an alkali-labile final product such as the Imz analogue,[30] *via* the hydrolytic decomposition of C(5)-hydroperoxide intermediate and/or the intramolecular cyclization of a transient Nfu species, resulting in a predominant oxidative strand cleavage at the ^{DMA}C site. Further detailed product analysis of the hole trapping reaction of ^{DMA}C in single-stranded DNA would be necessary for better understanding of the reactivity and detailed reaction mechanisms.

C(5)-substituent effects on the hole-trapping efficiency

We examined the electronic substituent effects on the hole-trapping ability of C(5)-modified cytosines. As an electronic substituent incorporated into cytosine at C(5), we focused on four typical types of dimethylamino, amino, methyl, and bromo groups. The ODN containing 5-aminocytosine (^{Am}C) was synthesized from the corresponding ODN bearing 5-bromocytosine (^{Br}C) according to previously reported methods.[31] Duplexes consisting of AQ-ODN1(G) with ^{32}P-labeled ODN1(X) (X = ^{DMA}C, ^{Am}C, 5-methylcytosine (^{M}C), normal C, and ^{Br}C) were photoirradiated, treated with hot piperidine, and then subjected to PAGE under the conditions described above. As shown in Fig. 4, strand cleavage at the G_{14} site was observed in each photoirradiated ODN, whereas the band intensities in ODN1(^{DMA}C) and ODN1(^{Am}C) were slightly lower than those observed in other ODNs. Intense strand cleavages at ^{DMA}C and ^{Am}C in ODN1(^{DMA}C) and ODN1(^{Am}C), respectively, were observed after 20-min irradiation; the corresponding cleavage band intensities were of a background level at the ^{M}C in ODN1(^{M}C), normal C in ODN1 (C), and ^{Br}C in ODN(^{Br}C) (Fig. 4, lanes 5, 9, 13, 17, and 21). These results clearly indicate that ^{DMA}C as well as ^{Am}C can efficiently trap the AQ-photoinjected holes in the positive-charge transfer through DNA duplexes. Incorporation of a strongly electron-donating group such as dimethylamino and amino groups, but not the methyl group, at the C(5) position of cytosine may substantially reduce oxidation potentials of the modified cytosines,[32] thereby leading to efficient hole trapping and subsequent strand cleavage at these sites. Considering the evidence that ^{Am}C itself was slightly degraded under the conditions of hot piperidine treatment (a basic condition at high temperature) (Fig. 4, lanes 2 and 6), the higher yield of strand cleavage at ^{DMA}C relative to ^{Am}C is most likely to originate from hole-transfer reaction and hole-trapping process in DNA. Thus, the ^{DMA}C is potentially applicable to an efficient molecular probe for investigation of the positive-charge transfer though DNA using gel electrophoresis.

Conclusions

In summary, we have characterized the AQ photosensitizer-injected hole transfer through DNA duplexes containing a ^{DMA}C base that is more readily one-electron oxidized into a radical cation intermediate than the other natural nucleobases. The AQ-sensitized photooxidation of duplexes containing ^{DMA}C demonstrated that photoinjected holes can migrate through the DNA bases to be trapped efficiently at the ^{DMA}C site, resulting in an enhanced oxidative strand cleavage at the ^{DMA}C site rather than at consecutive G sites, which would normally be a hotspot for the photosensitized oxidation. The ^{DMA}C radical cation intermediate formed by hole trapping may undergo specific hydration at C(6) and subsequent addition of molecular oxygen at C(5), leading to its degradation followed by strand cleavage at the ^{DMA}C site. This remarkable hole trapping and selective strand cleavage property of ^{DMA}C has prompted us to investigate hole-transfer mechanisms in more detail for higher-order DNA structures such as i-motifs consisting of cytosine-rich sequences. Further work along these lines is currently under way in our laboratories.

Experimental section

General

The reagents and solvents used were purchased from standard suppliers and used without further purification. The reagents for the DNA synthesizer were purchased from Glen Research.

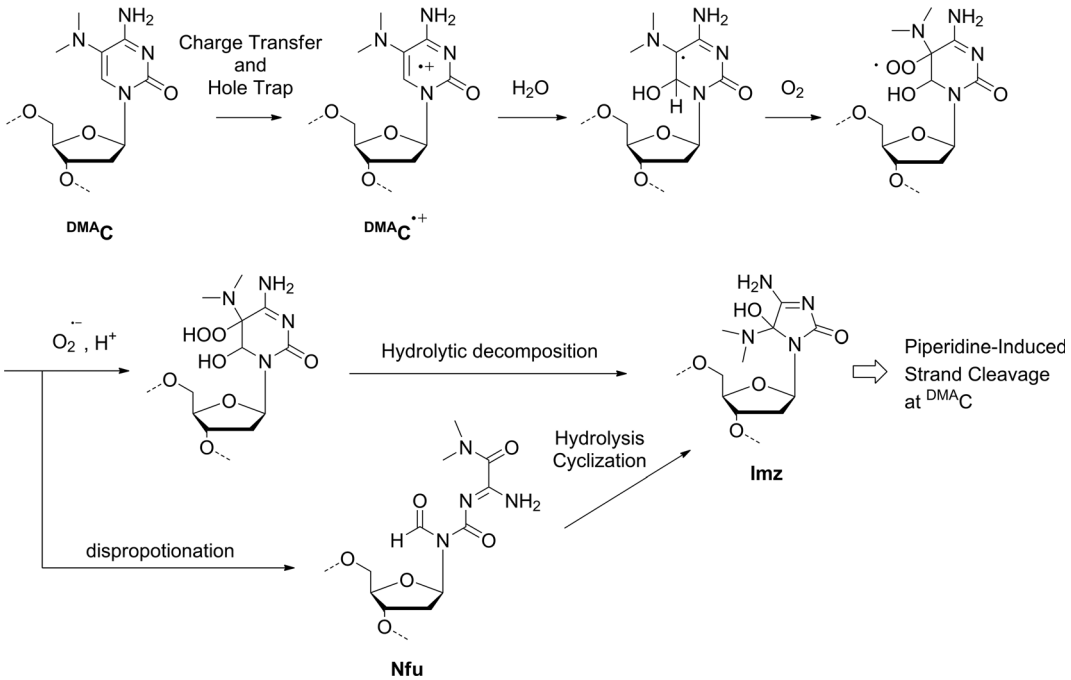

Scheme 2 A plausible photochemical reaction mechanism for exclusive strand cleavage at ^{DMA}C.

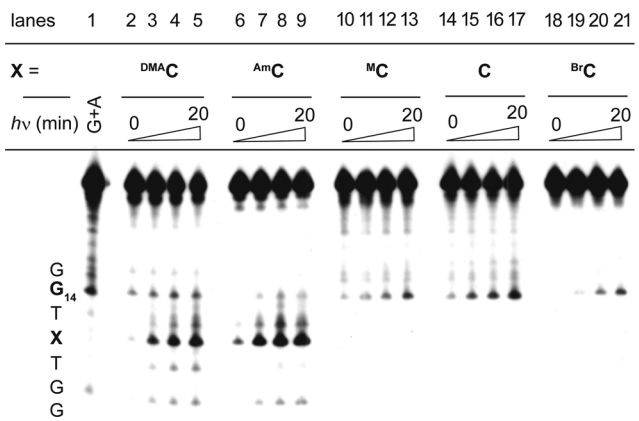

Fig. 4 Substituent effects on the hole-trapping induced strand cleavage at C(5)-modified cytosine. PAGE image of photoirradiated AQ-ODN1 (G)/ODN1(X) [X = ^{DMA}C (lanes 2–5), ^{Am}C (lanes 6–9), ^{M}C (lanes 10–13), C (lanes 14–17), and ^{Br}C (lanes 18–21)]. ODN duplexes were photoirradiated (0–20 min), followed by piperidine treatment under conditions identical to Fig. 2a. G+A indicates Maxam–Gilbert sequencing lane (lane 1).

Complementary ODNs were purchased from Invitrogen unless otherwise noted. Monomeric ^{DMA}C ($d^{DMA}C$) was prepared from 5-bromo-2′-deoxycytidine as detailed in ESI.† The NMR spectra were obtained on a JEOL JMN-AL-300 (300 MHz), a JEOL JMN-EX-400 (400 MHz), or a JEOL JMN-ECX-400 (400 MHz) spectrometer. *J* values are given in Hz. The FAB mass spectra were recorded on a JEOL JMS-SX102A spectrometer, using a nitrobenzyl alcohol or glycerol matrix. Matrix-assisted laser desorption ionization time-of-flight (MALDI–TOF) mass spectrometry of ODNs was performed on a JEOL LMS-ELITE MALDI–TOF mass spectrometer with 2′,3′,4′-trihydroxyacetophenone as the matrix. ESI–TOF mass spectra were obtained on a Bruker Daltonics micrOTOF focus-KE.

5′-(4,4′-Dimethoxytrityl)-5-dimethylamino-2′-deoxyuridine (2)

5′-(Dimethoxytrityl)-5-bromo-2′-deoxyuridine (**1**) was prepared as described elsewhere. A solution of **1** (3.66 g, 6.00 mmol) in 10 mL of 50% aqueous dimethylamine was sealed in a 10 mL vial and heated for 60 h at 60 °C. The residue was evaporated under reduced pressure. The crude product was purified by column chromatography (SiO_2, 100% ethyl acetate) to give **2** (1.79 g, 52%) as a white foam: ^{1}H NMR ($CDCl_3$, 400 MHz) δ 8.34 (s, 1H), 7.34–7.09 (9H), 6.76–6.75 (4H), 6.30 (t, 1H, J = 6.6 Hz), 4.42 (t, 1H, J = 2.9 Hz), 3.97 (d, 1H, J = 3.4 Hz), 3.71 (s, 6H), 3.36 (dd, 1H, J = 4.4, 10.4 Hz), 3.28 (dd, 1H, J = 3.2, 10 Hz), 2.34 (s, 6H), 2.29–2.14 (2H); ^{13}C NMR ($CDCl_3$, 400 MHz) δ 158.8, 149.0, 144.4, 139.5, 131.0, 130.2, 129.2, 128.9, 128.2, 127.9, 127.1, 113.3, 113.2, 85.5, 84.6, 72.6, 63.6, 55.3, 42.2, 38.8; FABMS m/z 574 [$(M + H)^+$]; HRMS calcd. for $C_{32}H_{36}N_3O_7$ 574.2553, found 574.2557.

3′-*O*-(*tert*-Butyldimethylsilyl)-5′-*O*-(4,4′-dimethoxytrityl)-5-dimethylamino-2′-deoxyuridine (3)

A solution of **2** (1.70 g, 3.00 mmol), *tert*-butyldimethylsilylchloride (900 mg, 5.97 mmol), and imidazole (820 mg, 12.0 mmol) in DMF (7 mL) was stirred for 6 h at room temperature. The reaction mixture was quenched by water and extracted with ethyl acetate. The organic layer was washed with brine, dried over Na_2SO_4, filtered, and concentrated. The crude product was purified by column chromatography (SiO_2, 100% ethyl acetate) to give **3** (1.95 g, 94%) as a white solid: ^{1}H NMR ($CDCl_3$, 400 MHz) δ 8.45 (s, 1H), 7.33–7.13 (9H), 6.74–6.71

(4H), 6.26 (dd, 1H, J = 5.9, 6.0 Hz), 4.34 (t, 1H, J = 3.2 Hz), 3.88 (dd, 1H, J = 3.2, 6.8 Hz), 3.69 (s, 6H), 3.32 (dd, 1H, J = 3.4, 10.2 Hz), 3.12 (dd, 1H, J = 3,8, 10.6 Hz), 2.35 (s, 6H), 2.20–2.15 (1H), 2.05–1.98 (1H), 0.77 (s, 9H), −0.04 (6H); ^{13}C NMR ($CDCl_3$, 400 MHz) δ 158.6, 149.0, 144.4, 135.5, 130.0, 129.1, 128.1, 127.9, 127.0, 113.2, 113.1, 86.4, 72.2, 62.9, 55.2, 42.3, 40.7, 25.6, 17.9, −4.7, −4.9; FABMS m/z 688 [$(M+H)^+$]; HRMS calcd. for $C_{38}H_{50}N_3O_7Si$ 688.3418, found 688.3412.

3′-*O*-(*tert*-Butyldimethylsilyl)-5′-*O*-(4,4′-dimethoxytrityl)-5-dimethylamino-2′-deoxycytidine (4)

A solution of **3** (1.94 g, 2.82 mmol), triethylamine (1.2 mL, 8.62 mmol), 4-dimethylaminopyridine (1.04 g, 8.46 mmol), and 2,4,6-triisopropylbenzenesulfonyl chloride (2.56 g, 8.46 mmol) in anhydrous acetonitrile (24 mL) was stirred at room temperature for 16 h. The mixture was cooled in an ice bath. Aqueous ammonia (28%, 35 mL) was added, and the mixture was stirred for 3 h at ambient temperature. The reaction mixture was concentrated under reduced pressure and was taken up in ethyl acetate. The organic layer was washed with brine, dried over Na_2SO_4, filtered, and concentrated. The crude product was purified by column chromatography (SiO_2, 4% methanol–chloroform) to give **4** (1.87 g, 97%) as a white solid: ^{1}H NMR ($CDCl_3$, 400 MHz) δ 7.55 (s, 1H), 7.54–7.23 (9H), 6.92–6.89 (4H), 6.46 (t, 1H, J = 6.8 Hz), 4.46 (dd, 1H, J = 6.6, 7.9 Hz), 4.05 (dd, 1H, J = 3.0, 7.0 Hz), 3.87 (s, 6H), 3.57 (dd, 1H, J = 3.2, 10.8 Hz), 3.26 (dd, 1H, J = 3.2, 10.8 Hz), 2.55–2.49 (1H), 2.38 (s, 6H), 2.17–2.10 (1H), 0.89 (s, 9H), 0.03 (6H); ^{13}C NMR ($CDCl_3$, 400 MHz) δ 163.4, 158.6, 144.4, 135.7, 135.5, 130.1, 129.8, 128.2, 127.9, 127.0, 113.2, 113.1, 86.3, 85.9, 72.0, 62.7, 55.2, 44.2, 42.0, 25.7, 17.9, −4.7, −5.0; FABMS m/z 687 [$(M+H)^+$]; HRMS calcd. for $C_{38}H_{51}N_4O_6Si$ 687.3578, found 687.3580.

3′-*O*-(*tert*-Butyldimethylsilyl)-5′-*O*-(4,4′-dimethoxytrityl)-*N*-acetyl-5-dimethylamino-2′-deoxycytidine (5)

A solution of **4** (1.87 g, 2.73 mmol), acetic anhydride (645 μL, 6.83 mmol), and 4-dimethylaminopyridine (167 mg, 1.37 mmol) in anhydrous pyridine (27 mL) was stirred for 12 h at room temperature. The reaction mixture was concentrated under reduced pressure, diluted with water, and extracted with ethyl acetate. The organic layer was washed with brine, dried over Na_2SO_4, filtered, and concentrated. The crude product was purified by column chromatography (SiO_2, 50% ethyl acetate–hexane) to give **5** (1.29 g, 65%) as a yellow solid: ^{1}H NMR ($CDCl_3$, 400 MHz) δ 7.82 (s, 1H), 7.43–7.24 (9H), 6.84–6.81 (4H), 6.26 (t, 1H, J = 6.6 Hz), 4.40 (dd, 1H, J = 3,4, 7.0 Hz), 4.02 (dd, 1H, J = 3.6, 6.8 Hz), 3.79 (s, 6H), 3.54 (dd, 1H, J = 3.2, 11.6 Hz), 3.22 (dd, 1H, J = 3.4, 10.6 Hz), 2.71 (s, 3H), 2.58–2.53 (1H), 2.29 (s, 6H), 2.12–2.05 (1H), 0.82 (s, 9H), −0.03 (6H); ^{13}C NMR ($CDCl_3$, 400 MHz) δ 158.7, 144.3, 135.5, 135.3, 130.1, 130.0, 129.1, 128.2, 127.9, 127.1, 113.2, 113.1, 86.7, 86.4, 71.7, 62.4, 44.8, 42.1, 25.7, 17.9, 4.7, −5.0; FABMS m/z 729 [$(M+H)^+$]; HRMS calcd. for $C_{40}H_{53}N_4O_7Si$ 729.3684, found 729.3701.

5′-*O*-(4,4′-Dimethoxytrityl)-*N*-acetyl-5-dimethylamino-2′-deoxycytidine (6)

Tetrabutyl ammonium fluoride (1.0 M, 3.5 mL, 3.5 mmol) was added to a solution of **5** (1.28 g, 1.76 mmol) in dry THF (24 mL) and the mixture was stirred at room temperature for 1 h. The reaction mixture was diluted with water and extracted with ethyl acetate. The organic layer was washed with brine, dried over Na_2SO_4, filtered, and concentrated. The crude product was purified by column chromatography (SiO_2, 5% methanol–chloroform) to give **6** (887 mg, 82%) as a yellow solid: ^{1}H NMR ($(CD_3)_2O$, 400 MHz) δ 7.68 (s, 1H), 7.37–7.13 (9H), 6.74–6.71 (4H), 6.28 (t, 1H, J = 7.8 Hz), 4.49 (1H), 4.12 (1H), 3.79 (s, 6H), 3.43 (dd, 1H, J = 3.6, 10.4 Hz), 3.24 (dd, 1H, J = 3.4, 10.2 Hz), 2.53 (s, 3H), 2.44–2.41 (1H), 2.38 (s, 6H), 2.23–2.20 (1H); ^{13}C NMR ($CDCl_3$, 400 MHz) δ 158.7, 144.3, 135.5, 135.3, 130.1, 130.0, 128.1, 127.9, 127.1, 113.2, 113.1, 86.9, 86.5, 86.4, 72.3, 63.4, 55.2, 44.8, 41.9, 26.3, 25.6; FABMS m/z 615 [$(M+H)^+$]; HRMS calcd. for $C_{34}H_{39}N_4O_7$ 615.2819, found 615.2821.

3′-(*N*,*N*-Diisopropylmethylphosphonamidite)-5′-*O*-(4,4′-dimethoxytrityl)-*N*-acetyl-5-dimethylamino-2′-deoxycytidine (7)

Compound **6** was coevaporated twice with anhydrous acetonitrile (1 mL). A solution of **6** (20 mg, 0.033 mmol), anhydrous diisopropylethylamine (16 μL, 0.10 mmol), and *N*,*N*-diisopropylmethylphosphonamidic chloride (7 μL, 0.033 mmol) in anhydrous acetonitrile (350 μL) was stirred for 4 h at room temperature. The reaction mixture was filtered and then placed on a DNA synthesizer.

Synthesis of ODNs

ODNs containing 5-dimethylaminocytosine were synthesized on an Applied Biosystems Model 3400 DNA/RNA synthesizer using standard phosphoramidite chemistry. ODNs containing the AQ sensitizer were prepared as in previously reported methods.[18b] ODN containing 5-aminocytosine was synthesized from ODN1(^{Br}C) (including 5-bromocytosine) as previously reported.[31] Synthesized ODNs were purified by reversed phase HPLC on an Inertsil ODS-3 (ϕ 10 mm × 250 mm, elution with a solvent mixture of 0.1 M triethylammonium acetate (TEAA) pH 7.0, linear gradient over 60 min from 0% to 30% acetonitrile at a flow rate 3.0 mL min^{-1}). The purity and concentration of modified ODN were determined by complete digestion with calf intestinal alkaline phosphatase, nuclease P1, and phosphodiesterase I. The synthesized ODNs were identified by MALDI–TOF mass spectrometry (for ODN1(^{DMA}C), AQ-ODN1(G), AQ-ODN1(I), and ODN2(T/^{DMA}C/T)) or ESI–TOF mass spectrometry (for ODN1(^{Am}C), ODN1(^{M}C), ODN1(^{Br}C), AQ-ODN2(A/G/A), AQ-ODN2(C/C/A), and AQ-ODN2(C/C/C)); ODN1(^{DMA}C) m/z 6241.48 (calcd. for [M − H]$^-$ 6240.15), ODN1(^{Am}C) m/z 886.5 (calcd. for [M − 7H]$^{7-}$ 886.6) ODN1(^{M}C) m/z 1034.2 (calcd. for [M − 6H]$^{6-}$ 1034.3), ODN1(^{Br}C) m/z 1045.2 (calcd. for [M − 6H]$^{6-}$ 1045.1), AQ-ODN1(G) m/z 6390.21 (calcd. for [M − H]$^-$ 6389.17), AQ-ODN1(I) m/z 6375.04 (calcd. for [M − H]$^-$ 6374.05), ODN2(T/^{DMA}C/T) m/z 5512.55 (calcd. for [M − H]$^-$ 5514.66), AQ-ODN2(A/G/A) m/z 1468.3

(calcd. for $[M - 4H]^{4-}$ 1468.4), AQ-ODN2(C/C/A) *m/z* 1452.3 (calcd. for $[M - 4H]^{4-}$ 1452.4), AQ-ODN2(C/C/C) *m/z* 1156.8 (calcd. for $[M - 5H]^{5-}$ 1156.9).

Fluorescence quenching

Quenching experiments of the fluorescence of the photosensitizer were carried out on a Shimadzu RF-5300PC spectrophotometer. The excitation wavelength for DCA (25 μM) was 390 nm and the monitoring wavelength was that corresponding to the respective emission band at 487 nm. The dynamic quenching rate constant k_q was determined by the Stern–Volmer equation: $I_0/I = 1 + k_q\tau_0$[2′-deoxyribonucleoside] where I_0/I is the ratio of the emission intensities in the absence and presence of 2′-deoxyribonucleoside and τ_0 is the lifetime of the singlet excited state of DCA (15.1 ns) in the absence of quencher.

Photooxidative cleavage reaction and PAGE analysis

ODNs were 5′-^{32}P-labeled by phosphorylation with 4 μL of [γ-^{32}P]ATP (PerkinElmer) and 4 μL of T4 polynucleotide kinase (Nippon Gene). The reaction mixtures were purified using QIAquick Nucleotide Removal Kit (QIAGEN) to remove excess unincorporated nucleotide. Complementary ODNs (1 μM) were annealed in 10 mM sodium cacodylate buffer (pH 7.0) containing 100 mM NaCl by heating to 90 °C, followed by slow cooling to room temperature. The samples were irradiated at 365 nm UV light with a transilluminator (FTI-20L, Funakoshi, Tokyo) at 20 °C on exposure to air. After irradiation, the DNA samples were precipitated by adding 10 μL of herring sperm DNA (1 mg mL^{-1}), 10 μL of 3 M sodium acetate and 800 μL of ethanol. The precipitated DNA was resolved in 50 μL of 10% piperidine (v/v), heated at 90 °C for 20 min, and concentrated. The radioactivity of samples was assayed using an Aloka 1000 liquid scintillation counter and the dried DNA pellets were resuspended in loading buffer (a solution of 80% formamide (v/v), 1 mM EDTA, 0.1% xylene cyanol, and 0.1% bromophenol blue). All reactions, along with Maxam–Gilbert G+A sequencing reactions, were heat denatured at 90 °C for 3 min and quickly chilled on ice. The samples (3–10 × 10^3 cpm) were loaded onto 20% polyacrylamide/7 M urea sequencing gels and electrophoresed at 1900 V for 60–90 min, transferred to a cassette, and stored at −80 °C with Fuji X-ray film (RX-U). The gels were analyzed using autoradiography with ATTO CS Analyzer (version 3.0). Individual yields were calculated relative to each total band intensity. The average of three independent measurements for each sample is indicated.

LC/ESI–MS analysis of one-electron photooxidation of 5-dimethylamino-2′-deoxycytidine sensitized by riboflavin

A solution of 5-dimethylamino-2′-deoxycytidine ($d^{DMA}C$) (200 μM) and riboflavin (200 μM) in 2 mM sodium cacodylate buffer (pH 7.0) containing 20 mM NaCl (total volume 100 μL) was exposed to 365 nm UV light at 0 °C and subjected to LC/ESI–MS analysis. LC/ESI–MS (negative mode) was performed with a Thermo Exactive equipped with a Thermo Accela LC system. The column eluents were monitored by UV absorbance at 260 nm. The solvent mixture of triethylammonium acetate buffer solution (0.1 M, pH 7.0) containing 5 vol% acetonitrile was delivered as the mobile phase.

Melting temperature (T_m) of hybridized ODNs

1 μM of appropriate ODNs was dissolved in 10 mM sodium cacodylate buffer (pH 7.0) containing 100 mM NaCl. UV melting curves were recorded on a JASCO-V630 spectrophotometer equipped with a multicell block and a Peltier temperature controller. Melting curves were obtained by monitoring the UV absorbance at 260 nm with the temperature being increased from 4 °C to 80 °C at a rate of 1 °C min^{-1}.

CD spectrum of hybridized ODNs

5 μM duplexes were dissolved in 10 mM sodium cacodylate buffer (pH 7.0) containing 100 mM NaCl. CD spectra of the solutions were recorded at 20 °C on a JASCO J-700 spectrophotometer, using a UV cell with 0.1 cm path length.

Acknowledgements

This research was supported financially by Grant-in-Aid for Young Scientists (B) from Japan Society for the Promotion of Science. We thank Prof. Teruyuki Kondo and Dr Yu Kimura (Advanced Biomedical Engineering Research Unit, Kyoto University) for ESI-TOF mass measurements.

Notes and references

1 (*a*) J. C. Genereux and J. K. Barton, *Chem. Rev.*, 2010, **110**, 1642–1662; (*b*) G. B. Schuster, *Acc. Chem. Res.*, 2000, **33**, 253–260; (*c*) B. Giese, *Acc. Chem. Res.*, 2000, **33**, 631–636; (*d*) F. D. Lewis, R. L. Letsinger and M. R. Wasielewski, *Acc. Chem. Res.*, 2001, **34**, 159–170.
2 (*a*) *Long-Range Charge Transfer in DNA I (Topics in Current Chemistry Vol. 236)*, ed. G. B. Schuster, Springer-Verlag, New York, 2004; (*b*) *Long-Range Charge Transfer in DNA II (Topics in Current Chemistry Vol. 237)*, ed. G. B. Schuster, Springer-Verlag, New York, 2004; (*c*) *Charge Transfer in DNA*, ed. H.-A. Wagenknecht, Wiley-VCH, Weinheim, 2005.
3 (*a*) I. Saito, T. Nakamura, K. Nakatani, Y. Yoshioka, K. Yamaguchi and H. Sugiyama, *J. Am. Chem. Soc.*, 1998, **120**, 12686–12687; (*b*) H. Sugiyama and I. Saito, *J. Am. Chem. Soc.*, 1996, **118**, 7063–7068; (*c*) V. Shafirovich, A. Dourandin and N. E. Geacintov, *J. Phys. Chem. B*, 2001, **105**, 8431–8435; (*d*) V. Shafirovich, J. Cadet, D. Gasparutto, A. Dourandin, W. D. Huang and N. E. Geacintov, *J. Phys. Chem. B*, 2001, **105**, 586–592.
4 J. D. Slinker, N. B. Muren, S. E. Renfrew and J. K. Barton, *Nat. Chem.*, 2011, **3**, 228–233.
5 T. G. Drummond, M. G. Hill and J. K. Barton, *Nat. Biotechnol.*, 2003, **21**, 1192–1199 and references therein.
6 A. Okamoto, T. Kamei and I. Saito, *J. Am. Chem. Soc.*, 2006, **128**, 658–662.
7 K. Kawai, H. Kodera, Y. Osakada and T. Majima, *Nat. Chem.*, 2009, **1**, 156–159.
8 A. Okamoto, K. Tanaka and I. Saito, *J. Am. Chem. Soc.*, 2003, **125**, 5066–5071.
9 (*a*) S. O. Kelly and J. K. Barton, *Chem. Biol.*, 1998, **5**, 413–425; (*b*) K. Nakatani, C. Dohno and I. Saito, *J. Am. Chem. Soc.*, 2000, **122**, 5893–5894.
10 H. Ikeda and I. Saito, *J. Am. Chem. Soc.*, 1999, **121**, 10836–10837.
11 A. Okamoto, K. Tanaka and I. Saito, *Bioorg. Med. Chem. Lett.*, 2002, **12**, 3641–3643.

12 (*a*) K. E. Augustyn, J. C. Genereux and J. K. Barton, *Angew. Chem., Int. Ed.*, 2007, **46**, 5731–5733; (*b*) F. Shao, K. Augustyn and J. K. Barton, *J. Am. Chem. Soc.*, 2005, **127**, 17445–17452.

13 (*a*) K. Nakatani, C. Dohno and I. Saito, *J. Am. Chem. Soc.*, 2001, **123**, 9681–9682; (*b*) C. Dohno, A. Ogawa, K. Nakatani and I. Saito, *J. Am. Chem. Soc.*, 2003, **125**, 10154–10155.

14 F. Shao, M. A. O'Neill and J. K. Barton, *Proc. Natl. Acad. Sci. U. S. A.*, 2004, **101**, 17914–17919.

15 H. Ding and M. M. Greenberg, *J. Am. Chem. Soc.*, 2007, **129**, 772–773.

16 (*a*) S. Fukuzumi, H. Miyao, K. Okubo and T. Suenobu, *J. Phys. Chem. A*, 2005, **109**, 3285–3294; (*b*) H. Yamada, K. Tanabe, T. Ito and S. Nishimoto, *Chem. Eur. J.*, 2008, **14**, 10453–10461.

17 S. L. Murov, I. Carmichael, G. L. Hug, *Handbook of Photochemistry,*, 2nd edn, Marcel Dekker, New York, 1993.

18 (*a*) B. Armitage, *Chem. Rev.*, 1998, **98**, 1171–1200; (*b*) S. M. Gasper and G. B. Schuster, *J. Am. Chem. Soc.*, 1997, **119**, 12762–12771; (*c*) R. P. Fahlman, R. D. Sharma and D. Sen, *J. Am. Chem. Soc.*, 2002, **124**, 12477–12485; (*d*) T. T. Williams, C. Dohno, E. D. A. Stemp and J. K. Barton, *J. Am. Chem. Soc.*, 2004, **126**, 8148–8158; (*e*) F. D. Lewis, A. K. Thazhathveetil, T. A. Zeidan, J. Vura-Weis and M. R. Wasielewski, *J. Am. Chem. Soc.*, 2010, **132**, 444–445.

19 Monomeric ^{DMA}C has the absorption band at wavelengths shorter than 350 nm. The photoirradiation at 365 nm can selectively excite AQ sensitizer.

20 K. Kawai, Y. Wata, M. Hara, S. Tojo and T. Majima, *J. Am. Chem. Soc.*, 2002, **124**, 3586–3590.

21 D. J.-F. Chinnapen and D. Sen, *J. Mol. Biol.*, 2007, **365**, 1326–1336.

22 S. Steenken and S. V. Jovanovic, *J. Am. Chem. Soc.*, 1997, **119**, 617–618.

23 T. Douki and J. Cadet, *Int. J. Radiat. Biol.*, 1999, **75**, 571–581.

24 Although we have not yet accomplished full assignment in the absence of comprehensive structural information on the photooxidation products by means of NMR spectroscopy, dImz may exist as the 5*R** and 5*S** forms, as in the case of 2′-deoxyribofuranosyl-5-hydroxy-5-methylhydantoin, a related degradation product to dImz[26].

25 We could not detect other photooxidation products under the present LC conditions. At the present stage, however, another possibility cannot be ruled out that other minor degradation products could be formed.

26 J. R. Wagner, J. E. van Lier, M. Berger and J. Cadet, *J. Am. Chem. Soc.*, 1994, **116**, 2235–2242.

27 (*a*) J. R. Wagner, C. Decarroz, M. Berger and J. Cadet, *J. Am. Chem. Soc.*, 1999, **121**, 4102–4110; (*b*) J. R. Wagner and J. Cadet, *Acc. Chem. Res.*, 2010, **43**, 564–571 and references therein.

28 In addition to predominant hydration at C(6) of ^{DMA}C$^{\cdot+}$, the minor pathway could be considered: the ^{DMA}C$^{\cdot+}$ may undergo competitive deprotonation of the exocyclic amine group.[27] In this context, other piperidine-stable oxidation products may be produced along with the formation of piperidine-labile Imz.

29 C. von Sonntag, *Free-Radical-Induced DNA Damage and Its Repair: A Chemical Perspective*, Springer-Verlag, Heidelberg, 2006.

30 The Imz site would be piperidine-labile in view of the fact that similar imidazolone analogs have been shown to be alkali-sensitive, resulting in strand cleavage at these sites. See. K. Kino, I. Saito and H. Sugiyama, *J. Am. Chem. Soc.*, 1998, **120**, 7373–7374.

31 (*a*) E. Ferrer, M. Wiersma, B. Kazimierczak, C. W. Müller and R. Eritja, *Bioconjugate Chem.*, 1997, **8**, 757–761; (*b*) C. Dohno, A. Okamoto and I. Saito, *J. Am. Chem. Soc.*, 2005, **127**, 16681–16684.

32 The ionization potentials of ^{DMA}C and ^{Am}C were estimated to be 8.58 and 8.64 eV, respectively, using the previously reported methods.[16b] This indicates that the oxidation potential of ^{DMA}C is not much different to that of ^{Am}C. The ionization potentials of ^{DMA}C and ^{Am}C were estimated by *ab initio* calculations at the B3LYP/6-31G* level. *Ab initio* calculations were performed for ^{DMA}C and ^{Am}C derivatives in which the sugar units were replaced by methyl groups.